Eur. Phys. J. D **1**, 47–52 (1998)

THE EUROPEAN PHYSICAL JOURNAL D

Vacuum ultraviolet photoionization of the 5d elements in the region of the 5p and 4f excitation

M. Martins, P. Sladeczek, K. Tiedtke, and P. Zimmermann[a]

Institut für Atomare und Analytische Physik, Technische Universität, Hardenbergstr. 36, 10623 Berlin, Germany

Received: 9 October 1997 / Accepted: 3 November 1997

Abstract. The results of recent VUV photoionization experiments of the 5d elements Ta, W, Re, Ir and Pt using atomic beam technique, excitation with monochromatized synchrotron radiation and detection of singly and doubly charged photoions are discussed. Special attention is given to the resonances caused by discrete transitions of the 5p and 4f electrons into the unfilled 5d subshells. As there is a crossover of the 5p and 4f levels along the series of the 5d elements the result is a complicated structure of the corresponding interacting resonances. The photoion spectra are compared with theoretical calculations carried out within the relativistic time dependent local density and the relativistic Hartree-Fock approximation.

PACS. 32.80.Fb Photoionization of atoms and ions – 32.80.Hd Auger effects and innershell excitation or ionization

1 Introduction

The use of monochromatized synchrotron radiation in the last decades has given an enormous impact on vacuum ultraviolet (VUV) photoionization experiments with metal atoms (see [1] and references therein). The 5d elements ($Z = 72-78$), however, until recently were excluded from such a development. The main reason was the difficulty in the production of free atoms due to the extreme temperatures in the range of 2300−3400 K required for the evaporation of the metals. Therefore, other techniques like the dual laser plasma technique were used to perform photoabsorption experiments with platinum and tungsten in the gas phase [2]. Here, the absorbing vapor and the backlighting continuum are produced by high power pulses of a synchronized twin laser system focused on solid targets. Only very recently the atomic beam technique with high temperature crucibles or with evaporating thin wires was successfully applied to the study of photoion yield spectra of the 5d elements after innershell excitation with monochromatized synchrotron radiation. Photoion yield spectra X^+ and X^{2+} of tantalum [3], tungsten [4], rhenium [3], iridium [5] and platinum [6] in the region of the 5p and 4f excitation are now available. Although corresponding data on hafnium and osmium are still missing, it is useful to give a survey of the present data especially with respect to common features and trends.

The interest of the VUV spectroscopy with the 5d elements is concentrated on the investigation of core resonances. Similar to the np $\rightarrow$ nd resonances of the 3d and 4d elements the most prominent resonances are due to transitions from the core electrons of the 5p subshell into the unfilled 5d subshell of the valence electrons. In addition to these 5p resonances, there is a crossover of the 5p and 4f levels along the series of the 5d elements. Therefore, we are confronted with the unique case that interacting core resonances originating from different subshells 5p and 4f can be studied in the same energy region.

This situation combined with the large number of resonances due to the unfilled 5d subshells is a challenge for theoretical calculations. As there are only very few results using advanced many-body theories [7] we have calculated photoionization cross sections of the 5d elements in the region of the 5p or 4f excitation and compare these results with the photoion yield spectra.

2 Fundamental processes in the photoionization of the 5d elements in the region of the 5p and 4f excitation

Vacuum ultraviolet photoionization of the 5d elements in the region of the 5p and 4f excitation (*ca.* 20-80 eV) is connected with several fundamental excitation and decay processes which are illustrated in the simplified energy scheme of Figure 1. The excitation takes place from the initial states of the configuration $4f^{14}\ 5p^6(5d,\ 6s)^n$ where $(5d,\ 6s)^n$ denotes possible configuration mixing of the type $5d^{n-2}\ 6s^2 \leftrightarrow 5d^{n-1}\ 6s \leftrightarrow 5d^n$ of the valence electrons. For atomic beam experiments of the 5d elements with the high evaporation temperatures the initial states are the ground state and thermally populated metastable states (see also Sect. 4). The excitation process can be divided into nonresonant and resonant processes.

[a] e-mail: kit@atom.physik.tu-berlin.de

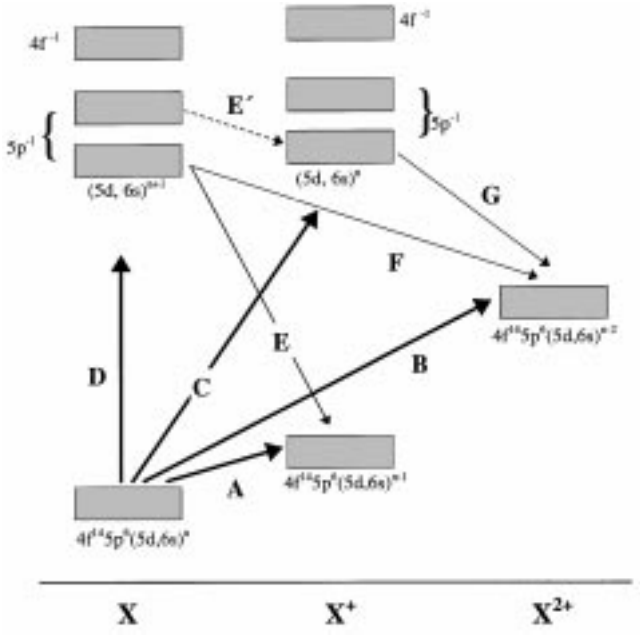

Fig. 1. Simplified level scheme of the 5d elements showing the different excitation and decay processes in the region of the 5p and 4f excitation/ionization. A: single photoionization of valence electrons 5d or 6s, B: double photoionization of valence electrons 5d or 6s, C: single photoionization of core electrons 5p or 4f, D: resonant photoexcitation of core electrons 5p or 4f into unfilled (5d, 6s) orbitals, E, E': single autoionization of the core excited atomic states, F: double autoionization of the core excited atomic states, G: Auger decay of the $5p^{-1}$ or $4f^{-1}$ hole states of X^+.

2.1 Non-resonant processes

The direct photoionization of the valence electrons 5d or 6s can take place as single photoionization (A) or double photoionization (B) yielding singly or doubly charged photoions X^+ or X^{2+}:

A :

$$X4f^{14}5p^6(5d,6s)^n + \hbar\omega \rightarrow X^+4f^{14}5p^6(5d,6s)^{n-1} + \epsilon\ell$$

B :

$$X4f^{14}5p^6(5d,6s)^n + \hbar\omega \rightarrow X^{2+}4f^{14}5p^6(5d,6s)^{n-2} + \epsilon\ell + (\epsilon\ell)'.$$

For photon energies above the 5p or 4f threshold the direct photoionization of a core electron 5p or 4f (C) is possible:

$$\text{C} : X4f^{14}5p^6(5d,6s)^n + \hbar\omega \rightarrow X^+4f^{14}5p^5(5d,6s)^n + \epsilon\ell$$
$$: X4f^{14}5p^6(5d,6s)^n + \hbar\omega \rightarrow X^+4f^{13}5p^6(5d,6s)^n + \epsilon\ell.$$

In this case the $5p^{-1}$- or $4f^{-1}$-hole states can subsequently decay by the emission of an Auger electron (G) into double charged photoions:

G :

$$X^+4f^{14}5p^5(5d,6s)^n \rightarrow X^{2+}4f^{14}5p^6(5d,6s)^{n-2} + (\epsilon\ell)_{\text{Au}}$$
$$X^+4f^{13}5p^6(5d,6s)^n \rightarrow X^{2+}4f^{14}5p^6(5d,6s)^{n-2} + (\epsilon\ell)_{\text{Au}}.$$

2.2 Resonant processes

In the case of the resonant processes the core electrons 5p or 4f are excited into unfilled orbitals of the valence electrons. The strongest processes are expected for the transitions into the 5d/6s-subshells (D):

$$\text{D} : X4f^{14}5p^6(5d,6s)^n + \hbar\omega \rightarrow X4f^{14}5p^5(5d,6s)^{n+1}$$
$$: X4f^{14}5p^6(5d,6s)^n + \hbar\omega \rightarrow X4f^{13}5p^6(5d,6s)^{n+1}.$$

The decay of the excited atomic states by autoionization can take place by single autoionization (E) or double autoionisation (F) into singly or doubly charged photoions:

$$\text{E} : X4f^{14}5p^5(5d,6s)^{n+1} \rightarrow X^+4f^{14}5p^6(5d,6s)^{n-1} + \epsilon\ell$$
$$: X4f^{13}5p^6(5d,6s)^{n+1} \rightarrow X^+4f^{14}5p^6(5d,6s)^{n-1} + \epsilon\ell$$

F :

$$X4f^{14}5p^5(5d,6s)^{n+1} \rightarrow X^{2+}4f^{14}5p^6(5d,6s)^{n-2} + \epsilon\ell + (\epsilon\ell)'$$
$$X4f^{13}5p^6(5d,6s)^{n+1} \rightarrow X^{2+}4f^{14}5p^6(5d,6s)^{n-2} + \epsilon\ell + (\epsilon\ell)'.$$

The decay route F of double autoionization with the simultaneous emission of two electrons giving rise to a continuous electron spectrum must be distinguished from the stepwise decay by the successive emission of two electrons with discrete energies like the decay route (E′ + G). Here, the emission of the first electron leads to high-lying X^+-states which subsequently decay into X^{2+} by Auger emission:

E′ + G :

$$X4f^{14}5p^5(5d,6s)^{n+1} \rightarrow X^+4f^{14}5p^5(5d,6s)^n + \epsilon\ell$$
$$\rightarrow X^{2+}4f^{14}5p^6(5d,6s)^{n-2} + (\epsilon\ell)_{\text{Au}}.$$

In photoion spectroscopy using time-of-flight techniques the photoion yield spectra of differently charged ions are measured simultaneously. Therefore, the ratio of X^{2+}/X^+ can be determined independently from fluctuations of the photon or atomic beam. This ratio can be used to get information about the different excitation and decay routes. For example, below the 5p or 4f thresholds and outside the resonances the ratio X^{2+}/X^+ gives directly the ratio of the ionization processes A and B. On the resonances it gives information about the ratio of the processes E and the sum (F + G).

As the photoion yield of X^{2+} cannot distinguish between the decay route F of double autoionization and the sequence E′ → G of single autoionization with subsequent Auger decay it is worthwhile to combine the results of photoion spectroscopy with those of photoelectron spectroscopy as this method can measure the sequential process but usually has difficulties with the quantitative determination of process F.

It should be noted that in the analysis above several simplifications were made. Radiative transitions were

completely neglected as the ratio of radiative to nonradiative transitions in this energy range usually is very small ($< 10^{-3}$) although in special cases the nonradiative transitions might be hindered by certain selection rules. Another simplification is the omission of triply charged photoions. They can be produced by processes like the direct triple photoionization or double photoionization plus single Auger decay or single photoionization plus double Auger decay of $X^+(5p, 4f)^{-1}$ states directly or *via* $X^{2+}(5p, 4f)^{-1}$ into X^{3+}. In the energy range of the experiments, however, the signals of X^{3+} compared with the sum ($X^+ + X^{2+}$) were below 5%. Therefore, these processes were neglected.

3 Measurements of the photoion yield spectra

The main problems in the production of free atoms of the 5d elements are connected with the high temperatures required for the thermal evaporation of the metals. If one considers a vapour pressure of about 1 Pa as a typical value inside the beam source to produce a particle density of about 10^{12} cm^{-3} in the interaction region with the photon beam, then the following temperatures are necessary: Hf (2710 K), Ta (3330 K), W (3500 K), Re (3300 K), Os (3230 K), Ir (2750 K) and Pt (2370 K). These temperatures and the lack of crucible materials (in fact, some of the 5d elements themselves like Ta or W are typical crucible materials) prevent the use of conventional atomic beam technique with high temperature sources heated by electron bombardment. The technique of directly heated thin wires can be used if the metals have an efficient sublimation rate below their melting points. Looking at the melting points of Hf (2500 K), Ta (3269 K), W (3683 K), Re (3453 K), Os (3318 K), Ir (2683 K) and Pt (2045 K) one realizes that with the exception of Pt (for which we used conventional atomic beam technique with a Ta crucible) the technique of evaporating thin wires can be applied. Nevertheless, one has to bear in mind that at these high temperatures a large number of electrons and ions are produced which can severely disturb the particle detection in photoionization experiments. Therefore, a careful shielding of charged particles was necessary. For the excitation of the atoms the monochromatized synchrotron radiation of the electron storage ring BESSY in Berlin was used. The light was dispersed by typical toroidal-grating monochromators and focused on the atomic beam. For intensity reasons only moderate resolving powers $E/\Delta E \simeq 100-200$ could be employed. The detection of the differently charged photoions was achieved by a conventional time-of-flight spectrometer with the pulsed-field technique. The photoion yield spectra X^+ and X^{2+} are published for Ta [3], W [4], Re [3], Ir [5] and Pt [6]. For comparison with the calculated photoionization cross sections (see Sect. 4) the sum spectra ($X^+ + X^{2+}$) of these elements are shown in compiled form in Section 5.

4 Calculations of the photoionization cross section

4.1 Relativistic time-dependent local density approximation (RTDLDA)

The experimental difficulties in the production of atomic beams for the 5d elements have their counterparts in the difficulties in the calculations of the photoionization cross sections due to the intrinsic problems which are connected with the large coupling possibilities of the unfilled 5d subshells, the inter-configuration mixing, in particular the (5d, 6s) mixing, and the competing resonances of the transitions from the different core subshells 5p and 4f. For a first survey of the spectra it is, therefore, of interest to use a method with less complexity. For that reason, we employed the relativistic time-dependent local density approximation (RTDLDA) with the DAVID code of Liberman and Zangwill [8] for the calculation of the photoionization cross section. In this method, the electron charge density which is calculated making use of the Dirac equation reacts to the external photon field. The change in the electron charge density gives rise to a dynamical polarizability which accounts for the corresponding photoabsorption cross section. Neglecting radiative decay processes this cross section can be identified with the photoionization cross section.

Figure 2 shows the results of the RTDLDA calculations for the 5d-elements Hf to Pt ($Z = 72-78$) including Au ($Z = 79$) with the filled 5d-subshell. At the beginning of the series (Hf and Ta) the cross sections are dominated by two distinct peaks which can be identified as the $5p_{3/2}$ and $5p_{1/2}$ resonances. From W on the $5p_{1/2}$ resonance vanishes which in this simplified (jj)-model can be explained by the filled $(5d_{3/2})^4$-subshell and the fact that the transitions $5p_{1/2} \rightarrow 5d_{5/2}$ are forbidden. Starting with Hf one can also see some smaller resonances at the low energy side below 20 eV. These resonances can be identified as the 4f transitions into the unfilled 5d orbitals. With increasing nuclear charge the positions of the 4f and 5p resonances are shifted to higher energies. The shifts of the 4f resonances, however, are much larger than those of the 5p resonances. Therefore, along the series there is a crossover of the resonances at about Re or Os. For that region one expects a large overlap and mixing of these resonances. In contrast to the 3p resonances of the 3d elements or the 4p resonances of the 4d element one has, therefore, the very interesting situation that for the 5d elements interacting resonances from the different subshells 5p and 4f can be studied systematically.

4.2 Hartree-Fock-calculations

Although the RTDLDA calculations show some trends of the 5p and 4f resonances there are, of course, severe drawbacks considering the resonances in more detail. Therefore, we used the Fano theory of autoionizing resonances [9] and the Cowan code [10] with relativistic extensions for the calculations of the photoionization cross section.

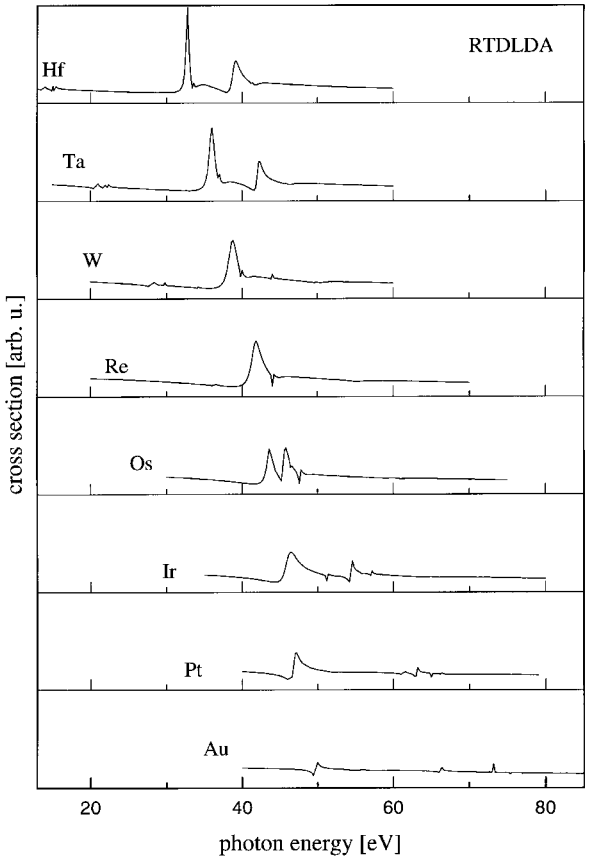

Fig. 2. Photoabsorption cross section (in arbitrary units) of the 5d elements in the region of the 5p and 4f excitation calculated with the relativistic version of the time-dependent local density approximation (RTDLDA). The different ordinates are not normalized to each other.

Here, the first step is the selection of the initial discrete states and the final discrete and continuum states.

The ground state configuration of the 5d elements usually is denoted by $5d^x6s^2$ [11] showing the successive filling of the 5d subshells. The ground state configuration $5d^96s$ for Pt and low lying states like $5d^56s\ ^7S_3$ for W or $5d^86s\ ^4F_{9/2}$ for Ir indicate, however, that due to the near energy degeneracy of the 5d and 6s orbitals one has to expect strong interconfiguration mixing between the configurations $5d^x6s^2, 5d^{x+1}6s$ and $5d^{x+2}$. Therefore, all these configurations, denoted by $(5d, 6s)^n$, were taken into account. For the initial states next to the ground state one has also to consider thermally populated states according to the temperatures in the range of 2300−3200 K for the production of the atomic beams.

For that reason, the initial states given in Table 1 were used (notation of Ref. [11]).

For the final states one has to distinguish between the discrete states and the continuum states. The transitions of the core electrons 5p or 4f into the unfilled valence subshells are modeled by the discrete configurations $5p^5(5d, 6s)^{n+1}$ or $4f^{13}(5d, 6s)^{n+1}$, the direct ionization of the valence electrons by the continuum configurations $(5d, 6s)^{n-1}\epsilon(p, f)$ and the direct ionization of the core electrons by the continuum configurations $5p^5(5d, 6s)^n\epsilon(s, d)$ or $4f^{13}(5s, 6s)^n\epsilon(d, g)$. The autoionization resonances are described by the configuration interaction of discrete and continuum states. In the case of independent resonances the Fano parameters Γ and q [9] are calculated, where Γ represents the decay width and the asymmetry parameter q measures the ratio of discrete to continuum transitions and is responsible for the shape of the resonance. For the 5d elements with their unfilled 5d subshells, however, there exists a large number of discrete transitions $5p^6(5d, 6s)^n \rightarrow 5p^5(5d, 6s)^{n+1}$ or $4f^{14}(5d, 6s)^n \rightarrow 4f^{13}(5d, 6s)^{n+1}$. As a consequence, one has to face the problem that many resonances overlap and interact with each other *via* the coupling of the discrete states with the same continua. Figure 3 shows as an example the large number of resonances in the calculated photoionization cross section of Ta [3]. Therefore, the extended theory of autoionization resonances (Mies formalism [12]) was used. The results of these calculations together with the photoion yield spectra are presented in the next section.

Table 1. Thermally populated states of the investigated 5d elements used as initial states for the photoionization process (notation of Ref. [11])

Element	Config.	(LSJ)	Energy (eV)	Rel. pop. (%)
Ta	$5d^36s^2$	$^4F_{3/2}$	0	48
$T \approx 3100$ K		$^4F_{5/2}$	0.249	27
		$^4F_{7/2}$	0.491	14
		$^4F_{9/2}$	0.697	8
W	$5d^46s^2$	$^5D_0$	0	15
$T \approx 3200$ K		$^5D_1$	0.207	21
		$^5D_2$	0.412	17
		$^5D_3$	0.599	17
		$^5D_4$	0.771	8
	$5d^56s$	$^7S_3$	0.366	28
Re	$5d^56s^2$	$^6S_{5/2}$	0	100
$T \approx 3000$ K				
Ir	$5d^76s^2$	$^4F_{9/2}$	0	78
$T \approx 2600$ K	$5d^86s$	$^4F_{9/2}$	0.352	15
Pt	$5d^96s$	$^3D_3$	0	46
$T \approx 2200$ K		$^3D_2$	0.096	20
	$5d^86s^2$	$^3F_4$	0.102	34

5 Experimental and theoretical results

The photoion yield spectra of singly and doubly charged photoions X^+ and X^{2+} for Ta, W, Re, Ir and Pt and the calculated photoionization cross sections in the relevant energy range of the 5p and 4f excitation are given in the recent publications ([3–6]). In order to get a general view of these results we have compiled the sum of the photoions

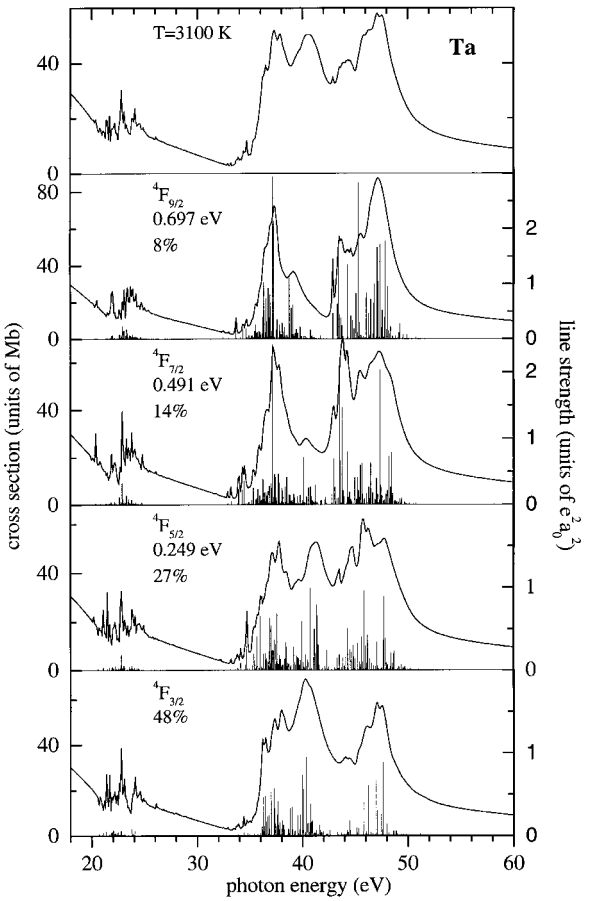

Fig. 3. Calculated photoionization cross sections of Ta [3] in the region of the 5p and 4f excitation showing the large number of resonances. At the top of Figure 3 the sum of the cross sections weighted according to the thermal population ($T = 3100$ K) of the four fine structure levels is depicted.

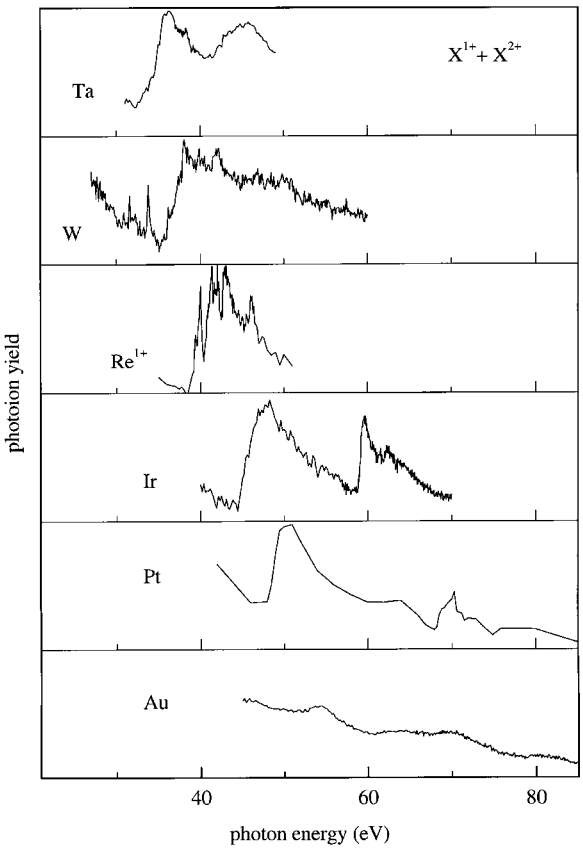

Fig. 4. Photoion yield spectra ($X^+ + X^{2+}$) (in arbitrary units) of Ta, W, Re, Ir, Pt and Au in the region of the 5p and 4f excitation/ionization (for Re only Re^+ is given). The different ordinates are not normalized to each other.

($X^+ + X^{2+}$) and the calculated photoionization cross sections in Figures 4 and 5. For Re only the photoion yield Re^+ is given as the values of Re^{2+} had too large uncertainties. The noble metal Au [13] is included to show the effect of the closed 5d subshell. The scale for the photoion yield of each element is arbitrary. In Figure 5 the calculated photoionization cross sections of these elements weighted according to the thermal population of the different initial states in the atomic beam are presented. The comparison of the experimental and theoretical results in Figures 4 and 5 shows that the main features of the photoion yield spectra are reproduced by the calculations. Looking back at the photoionization cross sections in Figure 2 which were obtained by the method of the time-dependent local density approximation (RTDLDA) one realizes that the multiplet structure which is not included in the RTDLDA code has an enormous influence on the spectrum.

The main features of the spectra are the dominant 5p resonances at the beginning of the series for Ta and W and the different shift of the 5p and 4f resonances with increasing nuclear charge which results in a crossover at about Re. The 5p resonances split into the two contributions of $5p_{1/2}$ and $5p_{3/2}$. Filling up the 5d orbitals the $5p_{1/2}$ contribution looses its influence which in the jj-coupling scheme can be explained by the increasing amplitudes of filled $(5d_{3/2})$-states and the forbidden transitions $5p_{1/2} \rightarrow 5d_{5/2}$. Both fine structure components $5p_{1/2}$ and $5p_{3/2}$ incorporate a large number of individual resonances (see Fig. 3) which overlap and interact with each other resulting in the broad features of Figure 5.

The multiplets of the 4f resonances show an even more complex structure than the 5p resonances in the spectra of Ir [5] and Pt [6] where the 4f states are already more strongly bound than the 5p states.

For Re in the region of the crossover of both resonances 5p and 4f there is a rather complicated situation where it seems extremely difficult to assign the resonances.

6 Summary

In summary we note that the VUV photoionization of the 5d elements in the region between 20 eV and 80 eV are dominated by strong resonances which are due to discrete transitions from the 5p subshell into the unfilled 5d/6s

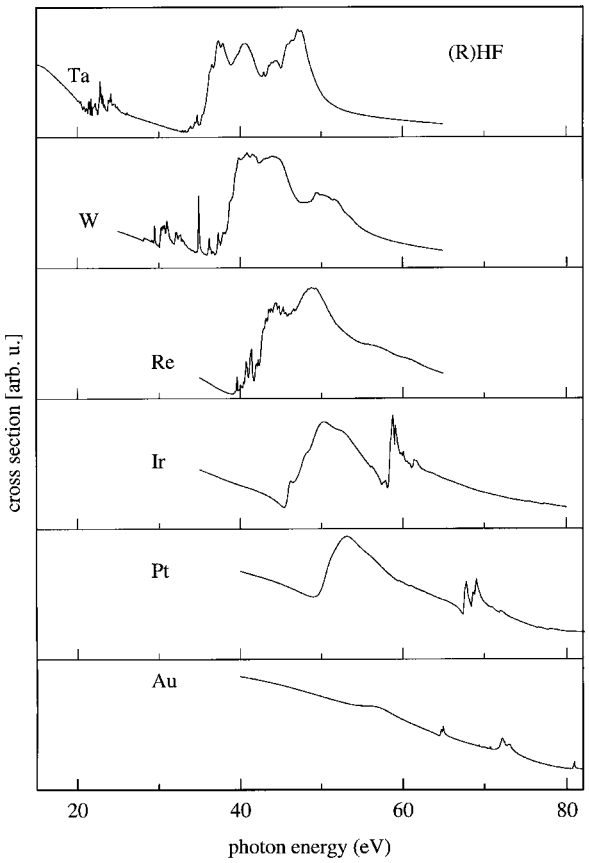

Fig. 5. Calculated photoionization cross section (in arbitrary units) of Ta, W, Re, Ir, Pt and Au in the region of the 5p and 4f excitation/ionization. The different ordinates are not normalized to each other.

orbitals. In contrast to the 3d and 4d elements with the corresponding 3p and 4p resonances there is also the possibility of discrete transitions from the 4f subshell with an energetic cross-over of the 5p and 4f levels along the series of the 5d elements. Both the experimental difficulties in the production of atomic beams due to the extreme evaporation temperatures and the theoretical complications due to the large number of interacting resonances are a challenge for further investigations.

We are thankful for financial support of the Deutsche Forschungsgemeinschaft. The assistance of the BESSY staff is gratefully acknowledged. This work was carried out with the partial support of the European Union under the HCM programme.

References

1. B. Sonntag, P. Zimmermann, Rep. Prog. Phys. **55**, 911 (1992).
2. J.T. Costello, E.T. Kennedy, B.F. Sonntag, C.L. Cromer, J. Phys. B: At. Mol. Phys. **24**, 5063, (1991).
3. M. Martins, P. Sladeczek, K. Tiedtke, P. Zimmermann, Phys. Rev. A **56**, 1329 (1997).
4. P. Sladeczek, H. Feist, M. Feldt, M. Martins, P. Zimmermann, Phys. Rev. Lett. **75**, 1483 (1995).
5. M. Martins, P. Sladeczek, K. Tiedtke, P. Zimmermann, Phys. Rev. A - Rapid commun. **55**, R8 (1997).
6. P. Sladeczek, M. Martins, M. Richter, K.-H. Selbmann, P. Zimmermann, J. Phys. B: At. Mol. Opt. Phys. **27**, 4123 (1994).
7. J. Boyle, Z. Altun, H.P. Kelly, Phys. Rev. A **47**, 4811 (1993).
8. D.A. Liberman, A. Zangwill, Comp. Phys. Commun., **32**, 75 (1984).
9. U. Fano, J.W. Cooper, Phys. Rev. **137** A1364 (1965).
10. R.D. Cowan, *The Theory of Atomic Spectra* (University of California Press, Berkeley 1981).
11. C.E. Moore, Natl., Bur. Stand. (U.S.), Circ. No 467 (U.S. GPO, Washington, D.C.), Vol. 3.
12. F.M. Mies, Phys. Rev. **175**, 164 (1968).
13. M. Martins, P. Sladeczek, P. Zimmermann, J. Phys. B: At. Mol. Opt. Phys. **29**, L754 (1996).